Agriculture, Ecosystems and Environment 324 (2022) 107725

Contents lists available at ScienceDirect

Agriculture, Ecosystems and Environment

journal homepage: www.elsevier.com/locate/agee

Nitrous oxide emission factors from an intensively grazed temperate grassland: A comparison of cumulative emissions determined by eddy covariance and static chamber methods

Rachael M. Murphy [a,b,*], Matthew Saunders [a], Karl G. Richards [b], Dominika J. Krol [b], Amanuel W. Gebremichael [b], James Rambaud [b], Nicholas Cowan [c], Gary J. Lanigan [b]

[a] Department of Botany, Trinity College Dublin, Dublin 2, Ireland
[b] Teagasc, Environment, Soils and Land-Use Department, Johnstown Castle, Wexford, Ireland
[c] UK Centre for Ecology and Hydrology, Bush Estate, Penicuik, Midlothian, UK

ARTICLE INFO

Keywords:
Grasslands
Eddy covariance
Grazing
Nitrous oxide
Emission factors

ABSTRACT

Quantifying nitrous oxide (N_2O) emissions from grazed pastures can be problematic due to the presence of hotspots and hot moments of N_2O from animal excreta and synthetic fertilisers. In this study, we quantified field scale N_2O emissions from a temperate grassland under a rotational grazing management using eddy covariance (EC) and static chamber techniques. Measurements of N_2O by static chambers were made for four out of nine grazing events for a control, calcium ammonium nitrate (CAN), synthetic urine (SU) + CAN and dung + CAN treatments. Static chamber N_2O flux measurements were upscaled to the field scale ($F_{CH\ FIELD}$) using site specific emission factors (EF) for CAN, SU+CAN and dung + CAN. Mean N_2O EFs were greatest from the CAN treatment while dung + CAN and SU + CAN emitted similar N_2O-N emissions. Cumulative N_2O-N emissions over the study period measured by $F_{CH\ FIELD}$ measurements were lower than gap-filled EC measurements. Emission factors of N_2O from grazing calculated by $F_{CH\ FIELD}$ and gap-filled were 0.72% and 0.96%, respectively. N_2O-N emissions were derived mainly from animal excreta (dung and urine) contributing 50% while N_2O-N losses from CAN and background accounted for 36% and 14%, respectively. The study highlights the advantage of using both the EC and static chamber techniques in tandem to better quantify both total N_2O-N losses from grazed pastures while also constraining the contribution of individual N sources. The EC technique was most accurate in quantifying N_2O emissions, showing a range of uncertainty that was seven times lower relative to that attributed to static chamber measurements, due to the small chamber sample size per treatment and highly variable N_2O flux measurements over space and time.

1. Introduction

Nitrous oxide (N_2O) is a potent greenhouse gas (GHG), with a global warming potential (GWP) 265 times higher than carbon dioxide (CO_2), over a 100 year lifespan (Pachauri et al., 2014). The largest contribution to global anthropogenic emissions of N_2O comes from the agricultural sector, and livestock production systems account for 30–50% of the total N_2O emissions from agriculture (Grossi et al., 2018). Sources of N_2O from agriculture include the use of chemical and organic nitrogen (N) fertilisers and animal excreta (Flechard et al., 2007), with nitrogen in these materials converted to N_2O either as a by-product of the microbial process of nitrification or as an intermediate product of denitrification (Davidson et al., 2000). Intensively managed grassland pastures require frequent N fertiliser applications to stimulate grass growth between rotational grazing events. As a result, a portion of the mineral N applied as fertiliser is added to pre-existing N pools deposited by animal excreta, which can substantially increase N_2O losses (Hyde et al., 2016). The spatial heterogeneity of urine and dung deposits (Carpinelli et al., 2020; Maire et al., 2018) can lead to 'hotspots' of N_2O, with N loading rates of 400–2000 kg N ha^{-1} in the affected areas (Jarvis et al., 1995). Such concentrations of N outweigh the uptake capacity of grass in the affected area, and this in conjunction with temporal variation in plant N demand and soil microclimatic conditions can further increase N_2O emissions from pastures (O'connell et al., 2004). As a result, it can be difficult to

* Corresponding author at: Department of Botany, Trinity College Dublin, Dublin 2, Ireland.
E-mail address: murphr32@tcd.ie (R.M. Murphy).

https://doi.org/10.1016/j.agee.2021.107725
Received 24 August 2021; Received in revised form 8 October 2021; Accepted 14 October 2021
Available online 25 October 2021
0167-8809/© 2021 The Authors. Published by Elsevier B.V. This is an open access article under the CC BY license (http://creativecommons.org/licenses/by/4.0/).

accurately quantify N_2O-N losses at the field scale from grazing systems.

The Intergovernmental Panel on Climate Change (IPCC) developed a standardised method for reporting N_2O emissions using a tiered approach based on emission factors (EFs) to quantify the amount of N_2O-N lost as a proportion of N applied to pastures (De Klein et al., 2010). The IPCCs default (Tier 1) EFs for mineral fertilisers (EF_1) is 1% with an uncertainty range of 0.3–3%, and for urine and dung N deposition on pasture, range and paddocks by grazing animals (EF_{3PRP}) is 2% with an uncertainty range of 0.7–6% (Eggleston et al., 2006). However, numerous studies have reported lower EFs for N_2O-N from urine and dung patches, ranging from 0.12% to 0.69% and 0.0027% to 0.19%, respectively (Chadwick et al., 2018; Hyde et al., 2016; Krol et al., 2016; Simon et al., 2018). As a result, the IPCC has revised the default EF_{3PRP} from 2% down to 0.6% (0–2.6%) and has disaggregated grazing EFs for dung at 0.13% (0–0.53%) and urine 0.77% (0.03–3.82%), as well as revising the EF_1 at 1.6% (1.3–1.9%) in wet temperate climates (Buendia et al., 2019). However, van der Weerden et al. (2021) reported higher mean emissions from dung and urine in wet temperate climates relative to the revised IPCC default values at 0.20% (0.17–0.27%) and 0.95% (0.88–1.03%). Default EFs reported by the IPCC use a Tier 1 methodology for reporting national N_2O emissions, however, there are large uncertainties surrounding these values. As a result, the IPCC encourages the use of country-specific (Tier 2) values which incorporate data on soil and climatic conditions, and farm management (Skiba et al., 2012). Ireland has developed Tier 2 disaggregated EFs for calcium ammonium nitrate (CAN) $EF_{1\ CAN}$ (1.4%), cattle urine, $EF_{3cattle\ –urine}$ (1.2%), and cattle dung, $EF_{3cattle\ –dung}$ (0.31%) (Harty et al., 2016; Krol et al., 2016; Roche et al., 2016).

The most commonly used method to quantify N_2O EFs is the chamber technique, accounting for 95% of the total field data on N_2O flux measurements (Rochette et al., 2008; Rochette, 2011; Wecking et al., 2020). Manually-operated chambers are the most commonly used method for investigating treatment effects on soil N_2O fluxes at small spatial scales (Clough et al., 2020; Krol et al., 2017; Maire et al., 2020). However, due to the highly heterogeneous nature of N_2O emissions from intensively managed pastures (Cowan et al., 2017), and the limited spatial and temporal resolution of single point static chamber measurements (Jones et al., 2011), the chamber technique is not always sufficient to characterise field-scale emissions of N_2O from grazing systems. In addition, static chamber flux measurements are often associated with large uncertainties due to artefacts that de-couple the chamber microclimate from external conditions. These include pressure differentials in the chamber headspace, as well as fluctuations in temperature and humidity (Hutchinson and Livingston, 2002; Rochette et al., 2008). Conversely, the eddy covariance (EC) technique provides real time, continuous measurements of the ecosystem to atmosphere exchange of N_2O that are integrated from multiple sources at the ecosystem scale. This technique is widely used to measure field scale N_2O emissions within agricultural landscapes (Cowan et al., 2016, 2020; Haszpra et al., 2018; Liang et al., 2018), however, as EC flux measurements represent a single non-replicated flux value that is integrated over a large spatial area, it does not provide disaggregated emissions from various emission sources. Therefore, in order to more accurately quantify emissions from grazed pastures, the use of static chamber and EC techniques in a complimentary fashion is advised (Cowan et al., 2017; Wecking et al., 2020). Flux estimates by EC can be used to quantify field scale emissions, while individual contributions from various sources can be determined by static chambers.

The objectives of this study were to 1) quantify the total field scale N_2O fluxes associated with a temperate grassland under a rotational grazing management system using the EC technique; 2) assess the contributions of background, fertiliser and animal excreta as determined by static chamber N_2O flux measurements and 3) evaluate how field scale emissions of background (i.e. no N applied), calcium ammonium nitrate (CAN), synthetic urine (SU) + CAN and dung+CAN compare with previously reported values in the literature.

2. Methods

2.1. Site description and experimental design

The study was carried out from January 1st to October 14th 2020 on a sandy loam soil site at the Teagasc Environmental Research Centre, Johnstown Castle, Co. Wexford in the south-east of Ireland (52.30°N, 6.40°W, 67 m above sea level. The mean annual air temperature and rainfall for this region over the last 10 years, is 10.1 °C and 1101 mm, respectively. The field site has a soil pH of 6.06, carbon (C), nitrogen (N) and phosphorus content of 3.52 (± 0.12%), 0.38 (± 0.01%) and 4.95 (± 0.20%), respectively. The field site is a perennial ryegrass (*Lolium perenne*) grassland, consisting of two paddocks (10 and 11) with a total area of 2.65 ha^{-1} (Fig. 1). Historically, paddock 10 was managed for silage production receiving 230 kg of CAN ha^{-1} in 2019 and 255 kg CAN ha^{-1} in 2018. Paddock 11 has been under both a silage production system (the same as paddock 10 in 2019) and managed for livestock production, grazed by Holstein Friesian dairy cows in 2018, receiving 277 kg ha^{-1} of urea coated with the urease inhibitor (n-Butyl) thiophosphoric triamide, (NBPT). In this study, there was a total of nine rotational grazing events occurring approximately every 21 days, with an average stocking density of 3.2 livestock units (LU) ha^{-1}, and six fertiliser applications of CAN (see Table 1). The prevailing wind direction is south-westerly, and the EC tower was set up in the North-East part of the field site to maximise the footprint (Fig. 1). During the measurement campaign, N_2O flux measurements were not available between 23rd March–27th March, and 13th June–15th June, for instrument maintenance. Additionally, field measurements of N_2O fluxes by EC were also not possible after the 14th of October due to delays in acquiring parts necessary for maintenance of the quantum cascade laser (QCL) as a result of the coronavirus (COVID-19) pandemic. The chamber trial plot was located in the south-west of paddock 10 (Fig. 1) and was 93 × 20 m in size and fenced off from surrounding grazing animals. The chamber trial plot consisted of two zones; a gas sampling zone (59 m × 10 m) and an adjacent soil sampling zone (36 m × 9 m). The grass within the trial plot (excluding inside chambers) was mechanically cut with an Etesia mower (Hydro 124 DL) while grass within the chamber was cut with a strimmer and removed following grazing outside the trial plot, within the paddocks. The gas sampling zone consisted of five different sub-trial zones for measuring N_2O emissions, and the soil sampling zone consisted of three different sub-trial zones for measuring soil mineral N (NH_4^+ and NO_3^-), both from four grazing events (see Table 1 for dates) - one in spring, two in summer and one in autumn in order to account for the temporal variability in N_2O fluxes. Each grazing sub-trial was designed in a randomised block of five replicate blocks for gas sampling or three replicate blocks for soil sampling, from four treatments – (1) control: without N application, (2) fertiliser in the form of CAN, (3) SU + CAN and (4) dung + CAN. Stainless steel collars and associated chambers were identical to those described by Harty et al. (2016), and collars were inserted into the soil 1.5 m apart both in length and width, in order to minimise cofounding effects between treatments. SU was prepared in the laboratory as outlined in De Klein et al. (2003), in 60 L batches that were stored at 4 °C prior to application. The N loading rate was equivalent to that of a standard cow urination (at approximately 500–700 kg N ha^{-1}) (Haynes and Williams, 1993). Dung was collected a week prior to application in the field immediately after defecation and stored as described above for SU. Composite sub-samples of SU and dung were analysed for total N using the LECO TruSpec high temperature Dumas Combustion system (St Joseph, Michican) and Ganimede analysis, respectively, and subsequent N loading rates were calculated for each application (Table 1). Dung and SU treatments were applied to the gas and soil measurement areas within the chamber trial plot when cows were grazing in strips within the South-West region of paddock 10, in front of the chamber trial plot. SU was applied using a water can to facilitate infiltration (Forrestal et al., 2017) at a volume of 1.8 L (Misselbrook et al., 2014) in an area of 0.16 m^2 within a chamber frame to reduce runoff through soil

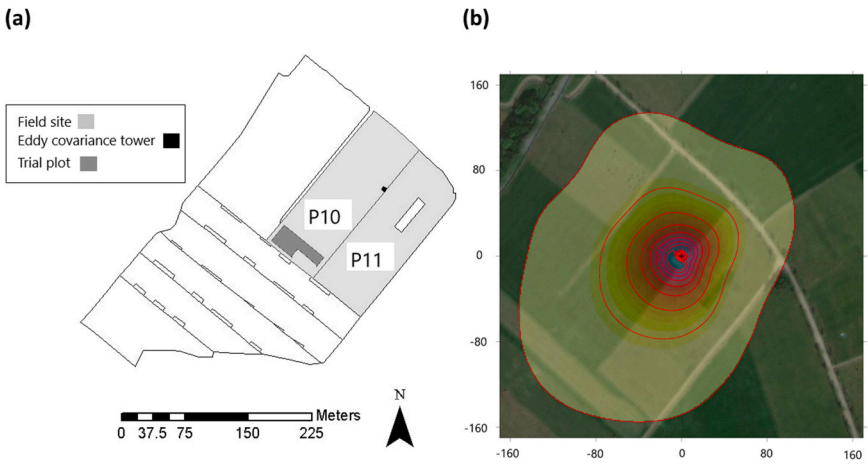

Fig. 1. (a) Map of the experimental field site at Johnstown Castle. Boundaries represent paddocks. P10 and P11 denote paddock 10 and paddock 11, respectively. The light grey paddocks represent the experimental field site (2.65 ha^{-1}) and the dark grey patch represents the chamber trial plot (0.09 ha^{-1}). The black square in P10 represents the eddy covariance (EC) tower and panel (b) shows the EC footprint for 2020 as calculated by the footprint model outlined in Kljun et al. (2015). The footprint contour lines represent 10–90% of the flux source in 10% increments. The axis represents distance (metres) from the EC tower (black cross).

Table 1
Management for the experimental site in 2020 and rates of application (kg nitrogen (N) ha^{-1}) for calcium ammonium nitrate (CAN), synthetic urine (SU) and dung that were applied to static chambers for four out of nine grazing events.

Date	Management	Application date	Application rate kg N ha^{-1}		
			CAN	SU	Dung
04/02/2020–10/02/2020	Grazing[1*+]	–	–	–	–
03/03/2020–22/03/2020	Grazing[1×]	03/03/2020	–	517	551
02/04/2020	Fertiliser[1×]	02/04/2020	50	–	–
10/04/2020–18/04/2020	Grazing	–	–	–	–
03/05/2020–10/05/2020	Grazing[2×]	04/05/2020	–	517	559
11/05/2020	Fertiliser[2×]	11/05/2020	40	–	–
25/05/2020–03/06/2020	Grazing3[×]	25/05/2020	–	517	405
03/06/2020	Fertiliser[3×]	03/06/2020	27	–	–
17/06/2020–24/06/2020	Grazing	–	–	–	–
29/06/2020	Fertiliser	–	20	–	–
09/07/2020–18/07/2020	Grazing	–	–	–	–
01/08/2020–12/08/2020	Grazing	–	–	–	–
14/08/2020	Fertiliser	–	27	–	–
31/08/2020–21/09/2020	Grazing[4×]	01/09/2020	–	542	355
14/09/2020	Fertiliser[4×]	14/09/2020	27	–	–

[×] Grazing events and CAN applications where N_2O emissions and mineral N were monitored for theduration of the experiment within the chamber trial plot. 1,2,3,4 is the number assigned to each grazing period, and is herein used in tables and figures.
[+] Due to wet soil conditions, spring grazing events were extremely sporadic and inconsistent, and as a result grazing 1 was extended from Februaryto March.

pores outside of the chamber. Dung was applied at 2 kg to a 30 cm diameter area within the chamber collar (Krol et al., 2016).

2.2. Chamber N_2O sampling and analysis

N_2O measurements were made using the closed static chamber technique as outlined in De Klein and Harvey (2015). Stainless steel 40 cm × 40 cm chambers were inserted into the ground at 5–10 cm depth at least three days prior to flux measurements. Chamber lids were 10 cm high creating an approximate headspace volume of 20–22 L. During sampling, chambers were closed for 30 min and flux measurements were taken at 0, 15 and 30 min from chamber closure through a rubber septum (Becton Dickinson, Oxford, UK) using a 10 ml polypropylene syringe (BD Plastiplak, Becton Dickinson) fitted with a hypodermic needle (BD, Microlance 3; Becton Dickinson). Gas samples were injected into a pre-evacuated 7 ml screw-cap septum glass exetainers (Labco, High Wycombe, UK). N_2O fluxes measurements occurred between 10:00 h and 14:00 h (UTC) to best reflect daily average N_2O emissions (Charteris et al., 2020). Measurements were made more frequently following the application of CAN, dung and SU inside chambers, with five sampling measurements for the first week, four sampling measurements in the second week post treatment application, two sampling measurements per week for following two weeks, then one sampling measurement a week for the following five weeks before reducing the measurement frequency to twice a month until week 17 post application, and thereafter once a month until the end of the experiment. N_2O concentrations were analysed using gas chromatography (GC) with a detection limit of 0.05 ppm (Scion 456-GC, Bruker Inc., Kirkton Campus Livingston, UK) equipped with an electron capture detector. For each series of gas samples from a chamber, the hourly flux (F_{CH}) (μg N_2O m^{-2} h^{-1}) was calculated using the following Eq. (1).

$$F_{CH} = \left(\frac{\Delta C}{\Delta T}\right) \quad x \quad \left(\frac{M \quad x \quad P}{R \quad x \quad T}\right) x \quad \left(\frac{V}{A}\right) \tag{1}$$

Where ΔC/ΔT is the change in headspace concentration of N_2O (ppbv) during the enclosure period in hours calculated by linear regression, M is the molecular weight of N_2O (44.01 g mol^{-1}), P and T are the atmospheric pressure (Pa) and temperature (K) at the time of gas sampling, respectively, R is the ideal gas law constant (8.314 J K^{-1} mol^{-1}), V is the headspace volume in a closed chamber (m^3) and A is the ground area enclosed by the chamber (m^2). Linearity of N_2O accumulation within the chamber headspace was checked from three headspace samples per chamber (De Klein and Harvey, 2015).

2.3. Eddy covariance flux measurements

The EC system was equipped with a 3-D sonic anemometer (CSAT-3, Campbell Scientific Ancillary, Logan, UT, USA) mounted at 2.2 m to measure fluctuations in the 3-D wind components at a frequency of 10 Hz. Concentrations of N_2O and H_2O were measured at 10 Hz by a quantum cascade laser (QCL) (Los Gatos Research, California, USA), with a detection limit of 0.03 ppb over a 30 min period. The QCL was housed in a temperature controlled trailer adjacent to the EC mast. The inlet line into the QCL was a 10 m long, 10 mm inner diameter perfluoroalkoxy (PFA) tube with an airflow rate of approximately 30–35 standard L min^{-1}, controlled by an external dry scroll vacuum pump (XDS35i, Edwards, West Sussex, UK). Two in line 2 μm filters (SS-4FW4-2, Swagelok™) were fitted on the PFA tube and an additional 2 μm and 10 μm (Los Gatos Research, California, USA) filters were fitted within the QCL at the entrance of the inlet tubing and upstream of the internal pump, respectively. The air inlet into the QCL sensor was placed in the same horizontal axis, 30 cm apart from the sonic anemometer reference. The QCL contained an internal temperature regulator that maintained the cell temperature to 34 °C ± 0.5 °C and the cell pressure was set at 85 torr. Environmental variables at the EC site were measured using a range of sensors including an air temperature and relative humidity probe (HMP155C, Campbell Scientific, Logan, UT, USA), tipping bucket rain gauge (Young, Michigan, USA), two net radiation sensors (NR-Lite, Kipp and Zonen, Delft, The Netherlands), two self-calibrating soil heat flux plates that were installed at 5 cm soil depth (HFP01SC, Hukseflux, Delft, The Netherlands), photosynthetic active radiation (PAR) (PQS1, Kipp and Zonen, Delft, The Netherlands) and averaging soil temperature probes (TCAV-L, Campbell Scientific, Logan, UT, USA) that were installed at 2 cm and 6 cm depth above the soil heat flux plates. Time domain reflectometers (CS616, Campbell Scientific, Logan, UT, USA) measured soil volumetric water content (VWC) in the upper 15 cm of soil. Soil bulk density (0–10 cm) was measured prior to the experiment by a core method (USDA, 1999) in order to calculate the water filled pore space (WFPS %) as outlined in Linn and Doran (1984). Data from the EC system was recorded and collected weekly from the CR3000 micrologger (Campbell Scientific, Logan, UT, USA). EC fluxes of N_2O (F_{EC}) were calculated over 30 min intervals using the Eddypro software version 7.0.4 (www.licor.com/eddypro), based on the covariance between the N_2O concentration (N) and wind speed (w) Eq. (2):

$$F_{EC} = \overline{w'N'} \tag{2}$$

Raw half-hourly EC N_2O flux measurements were initially processed for amplitude resolution, drop-outs, absolute limits, skewness and kurtosis, as outlined in Vickers and Mahrt (1997). To compensate for the tilt of the sonic anemometer, double rotation was performed to nullify the average cross-stream and vertical wind component (Kaimal and Finnigan, 1994). Low and high pass spectral corrections were accounted for using the analytical methods described by Fratini et al. (2012) and Moncrieff et al. (2004), respectively. The covariance maximisation procedure was used to calculate the time lag for N_2O as described in Cowan et al. (2020). Flux data were removed if less than 70% of the flux contribution came from outside of the field site (Kormann and Meixner, 2001) and if flux values were < -0.1 μmol N_2O m^{-2} s^{-1}. Additional filtering for bad quality fluxes were derived from Cowan et al. (2020). Missing N_2O fluxes were gap-filled using a multi-variate linear model including the previous and next measured value in the dataset, and air and soil temperature, WFPS and rainfall over 2, 12, 24, 48 and 100 h periods. Gap-filled EC N_2O flux measurements presented in this study are expressed as a daily average.

2.4. Soil sampling and analysis

Soil was sampled on 45 occasions during the experimental period, once before treatment application and once a week for the next eight weeks following treatment application, in a randomised block design sampling area adjacent to the gas sampling area within the trial plot. The soil cores were taken using a hand core at 10 cm depth and 15 mm diameter and then mixed, homogenised and processed in the laboratory for ammonium (NH_4^+), nitrate (NO_3^-) and gravimetric moisture content within 24 hrs. Soil mineral N concentrations were analysed from a 20 g sample of freshly sieved soil (< 4 mm), extracted with 100 ml KCL (1 M) and analysed colorimetrically using an Aquakem 600 discrete analyser (Thermo Electron OY, Vantaa, Finland) for NH_4^+-N (Standing Committee of Analysts, 1981) and NO_3-N (Askew, 2012) concentrations. The gravimetric moisture content was determined by oven-drying samples at 105 °C for 24 h.

2.5. Data analysis

Data analysis was carried out on the statistical software R (Team, 2020). Hourly chamber fluxes were assumed to be representative of daily emissions and were used to calculate the daily mean N_2O flux. In order to approximate the total N_2O produced from CAN, dung+CAN and SU+CAN, cumulative fluxes were calculated using loess regressions. Cumulative chamber N_2O fluxes were used to derive EFs for each treatment and each grazing Eq. (3). EFs represent the % of N_2O-N emitted from dung+CAN, SU+CAN or CAN applied

$$EF = \left(\frac{[N_2O \quad _{Treatments} - N_2O \quad _{Control}]}{N \quad applied} \right) * 100 \tag{3}$$

Where N applied is the N applied from the treatment (CAN, SU or dung) (kg N ha^{-1} yr^{-1}), $N_2O_{Treatments}$ is the cumulative N_2O emissions (kg N_2O-N ha^{-1} yr^{-1}) from dung+CAN, SU + CAN or CAN per grazing and $N_2O_{Control}$ is the average N_2O emission (kg N_2O-N ha^{-1} yr^{-1}) from the control treatment per grazing cumulated over the duration of the grazing event (Cowan et al., 2019). The IPCC Tier 1 methodology assumes a standard, annual EF (Pachauri et al., 2014), however, in this study treatment EFs were calculated over 29, 34, 27 and 28 days for grazing 1, 2,3 and 4 respectively. Therefore the EFs reported in this study are considered partial EFs, but are unlikely to vary from those measured at annual scales as N_2O emissions from control plots were deducted from N_2O emissions measured from treatment plots and over a range of temporal conditions (Maire et al., 2020).

A direct comparison between chamber and EC cumulative flux measurements for a 288 day period was possible by upscaling chamber measurements to the paddock scale. Chamber fluxes were upscaled ($F_{CH\ FIELD}$) by using EF from grazing 1–4 for each treatment (Table 3) (Eq. (4)).

$$F_{CH \quad FIELD} = \frac{Napp * EF}{100} \tag{4}$$

Where Napp is the N applied to the field (kg N ha^{-1}) and EF is the mean emission factor (%) calculated over the 4 grazing events for a given treatment. For livestock emissions of dung and urine, the Napp at the field scale ($Napp_{Livestock}$) (Eq. (5)) was determined by the N rate per patch (N_{patch}) and total number of daily patches ($Patch_{daily}$)

$$Napp_{Livestock} = Patch_{daily} \quad * N_{patch} \tag{5}$$

Where $Patch_{daily}$ (Eq. (6)) was calculated as,

$$Patch_{daily} = grazing \quad duration * herd \quad size * Patch_{no.} \tag{6}$$

where the grazing duration is the time cows spent grazing (h^{-1}), herd size quantified the number of cows grazing, $Patch_{no.}$ was the number of urine or dung patches specified for Holstein Friesian at 7.5 (Dennis et al., 2011) and 10.9 (White et al., 2001) per grazing day (21 h^{-1}), and N_{patch} (Eq. (7)) was quantified as

$$N_{patch} = Area_{patch} * \mu(Napp) \tag{7}$$

Where $Area_{patch}$ was the wetted surface for each deposition event, with 0.33 m^{-2} for urine (Dennis et al., 2011) and 0.12 m^{-2} for dung (Wilkinson and Lowrey, 1973) and μ(Napp) was the average N application rate for dung or SU from grazing 1–4 (Table 1) quantified as 443 kg N ha^{-1} and 554 kg N ha^{-1}, respectively.

Literature values for EFs of CAN (Harty et al., 2016), dung (Krol et al., 2016) and urine (Maire et al., 2020) were used to calculate cumulative emissions for comparison with this study as these studies were carried out at the same experimental site or sites within the same research farm (Table 3) (Fig. 4). These literature background cumulative emissions were also derived from a previous study on the same experimental site (Krol et al., 2017).

The 95% confidence interval (2σ) was used to determine if differences between N_2O emissions measured by chambers from individual treatments were significantly different from zero. The Shapiro-Wilk Test was used to assess normality in the N_2O flux datasets (both chambers and EC) using the stats package in R. Where the p value from the Shapiro-Wilk Test was greater than 0.05, the dataset was deemed normally distributed. Where the p was less than 0.05, i.e. the dataset was log normally distributed, measured N_2O fluxes were transformed to a normal distribution using the bestNormalize package in R (Peterson and Cavanaugh, 2019) for statistical analysis. Linear correlations between daily field scale N_2O fluxes by EC and rainfall and WFPS were performed to determine significance and the coefficient of determination (R^2). A repeated measures ANOVA was used to investigate interaction affects between chamber N_2O fluxes, treatment and time using the car package in R.

3. Results

3.1. Weather and eddy covariance N_2O flux data

Daily weather and field-scale N_2O flux data measured at the EC station between January 1st and October 14th 2020 is shown in Fig. 2. Daily mean air temperature ranged from 2.2 °C in February to 19.8 °C in August (Fig. 2a), which represented a cooler February and warmer August, relative to the 10 year mean (2009–2019) for those respective months (Table 1A). Soil temperature at 6 cm depth was greatest in June and lowest in January with values of 20.3 °C and 2.1 °C (Fig. 2a), respectively, which represented a warmer June and colder January compared to the 10 year mean for these months (Table 1A). Cumulative rainfall for the experimental period was 502 mm (Fig. 2b). Rainfall was most frequent in the winter and spring resulting in high WFPS (≥ 60%) but the heaviest events (> 15 mm daily) were observed in the summer and autumn. Extended dry periods (< 50% WFPS) were observed between May 25th and 18th June (Fig. 2c).

Peaks in daily N_2O emissions principally occurred post-fertiliser application or during grazing, but both emission intensity and timing were strongly mediated by both temperature and rainfall (Fig. 2a, b, d). A bell-curve relationship was observed with N_2O fluxes and WFPS, and N_2O emissions were greatest within a WFPS range of 60–70% (Fig. 1A). Daily mean N_2O emissions were greatest within a soil temperature range of 15–20 °C (Fig. 1A) but were only significantly correlated ($p < 0.05$) with soil temperature during the February ($r^2 = 0.63$) and March ($r^2 = 0.29$) grazing (Table 2A). Daily emissions of N_2O were significantly correlated with rainfall ($p < 0.05$) for grazing events' in February ($r^2 = 0.84$), March ($r^2 = 0.14$), May ($r^2 = 0.67$), and June ($r^2 = 0.47$) (Table 2A). Emissions of N_2O were also significantly correlated with WFPS ($p < 0.05$) during grazing events' in February ($r^2 = 0.66$), March ($r^2 = 0.20$), April ($r^2 = 0.58$), June ($r^2 = 0.76$) and July ($r^2 = 0.34$) (Table 2A). Rainfall prior and during the June grazing co-occurred with fluctuations in N_2O emissions ranging from 0.05 nmol N_2O-N m^{-2} s^{-1} to 2.9 nmol N_2O-N m^{-2} s^{-1}. The highest emission event observed was 9.9 nmol N_2O-N m^{-2} s^{-1}, following a series of small rainfall events (< 0.6 mm) and increasing WFPS from 48% to 61%. No peaks were observed during grazing periods in early spring (February-March) where rainfall was consistent (WFPS > 50%) and soil temperatures were < 10 °C.

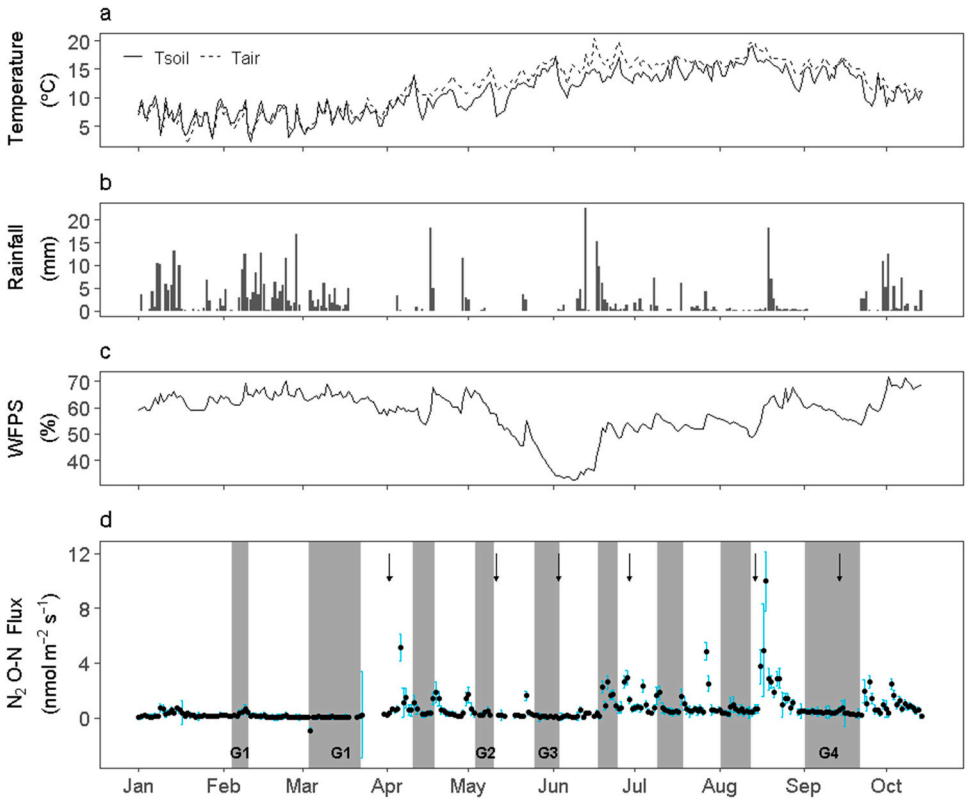

Fig. 2. Panels (a)–(c) represent the daily mean soil temperature (Tsoil) (solid line) and air temperature (Tair), (dashed line), daily sums of rainfall and daily mean water-filled pore space (WFPS), respectively. Panel (d) represents daily average N_2O-N fluxes measured by eddy covariance where blue lines represent the 95% confidence interval. The grey back drop represents grazing periods where G1–G4 represents grazing events 1–4 that were measured for N_2O flux measurements by static chambers. Black arrows mark the date of fertiliser applications.

Table 2
Cumulative N_2O-N emissions and partial emission factors (EF) measured by static chambers for each treatment per grazing (n = 5 per treatment per grazing). Treatments included no N applied (Control), fertiliser in the form of calcium ammonium nitrate (CAN), synthetic urine (SU) and CAN applied together and dung and CAN applied together.

Grazing	Cumulative N_2O-N emissions								Partial N_2O-N EF					
	Control		CAN		SU + CAN		Dung + CAN		CAN		SU + CAN		Dung + CAN	
	kg N ha^{-1}	95% C.I.	kg N ha^{-1}	95% C.I.	kg N ha^{-1}	95% C.I.	kg N ha^{-1}	95% C.I.	%	95% C.I.	%	95% C.I.	%	95% C.I.
1	0.27	0.21	3.06	1.48	7.51	1.83	2.53	0.95	5.58	2.70	1.28	0.31	0.38	0.14
2	0.07	0.02	0.71	0.06	1.64	0.36	6.12	1.47	1.60	0.14	0.28	0.06	1.01	0.24
3	0.08	0.03	0.68	0.17	1.69	0.23	1.36	0.25	2.22	0.57	0.30	0.04	0.30	0.06
4	0.06	0.01	0.53	0.06	2.84	0.33	3.37	0.64	1.73	0.18	0.49	0.06	0.87	0.16
Mean	0.12	0.07	1.24	0.44	3.42	0.69	3.35	0.83	2.78	0.90	0.59	0.12	0.64	0.15

3.2. N_2O emissions from grazing treatments

Cumulative N_2O-N emissions and partial N_2O-N EFs measured by chambers from control, CAN, SU + CAN and dung+CAN for grazing events' 1–4 are shown in Table 2. There was a significant interaction between N_2O emissions and time and treatment ($p < 0.001$). The control treatment (no N applied) showed low cumulative emissions with a mean value of 0.12 ± 0.07 kg N ha^{-1}. Mean cumulative N_2O-N emissions were significantly lower ($p < 0.05$) for CAN (1.24 ± 0.44 kg N ha^{-1}) compared to SU+CAN (3.42 ± 0.69 kg N ha^{-1}) and dung+CAN (3.35 ± 0.83 kg N ha^{-1}). The N loading applied to the treatments varied with grazing due to differences in CAN rates and the N contents of dung and SU (Table 1). EFs were calculated for comparability between treatments (Table 2). Over the four grazing events, mean EFs from CAN were greatest (2.78 ± 0.90%), followed by dung+CAN (0.64 ± 0.15%) and SU+CAN (0.59 ± 0.12%). The CAN treatment had consistently higher EFs in each grazing event compared to SU+CAN and dung + CAN treatments. The EF for SU+CAN was greater than the EF for dung + CAN in grazing 1 (spring) at 1.28 ± 0.31% and 0.38 ± 0.14%, respectively. The dung+CAN treatment showed higher EFs compared to SU+CAN in grazing 2 during summer (dung+CAN 1.01 ± 0.24%; SU+CAN 0.28 ± 0.06%) and in grazing 4 during autumn (dung+CAN 0.87 ± 0.16%; SU+CAN 0.49 ± 0.06%). In grazing 3 during summer EFs for the SU+CAN and dung+CAN treatments were the same at 0.30 ± 0.04/0.06%.

3.3. Field scale cumulative N_2O emissions by eddy covariance and upscaled chambers

Upscaling chamber fluxes (Section 2.5) to the paddock scale allowed for a direct comparison with EC fluxes on a daily basis. Cumulative N_2O emissions over 288 days of the grazing period were calculated for gap-filled EC fluxes and $F_{CH\ FIELD}$. Emissions of 5.16 ± 2.04 kg N ha^{-1} measured from $F_{CH\ FIELD}$ compared well with EC emissions of 6.62 ± 0.33 kg N ha^{-1} showing a similar cumulative pattern over time (Fig. 3). $F_{CH\ FIELD}$ emissions were consistently higher than EC emissions following the April grazing, up until the August fertiliser application where an increase in EC emissions was observed. The largest proportion of the total $F_{CH\ FIELD}$ emissions (5.51 kg N ha^{-1}), at 19.67% were observed from management in April, followed by management activities in September at 14.20% and March at 12.56% (Table 3). The February grazing accounted for the lowest proportion of the total cumulative flux at 1.34%, while emissions from early and late May, June, July and August accounted for 8.18%, 10.14%, 9.34%, 9.61% and 11.92% of the total $F_{CH\ FIELD}$ emissions, respectively (Table 3).

4. Discussion

4.1. Temporal trends in N_2O emissions

Mean daily N_2O emissions observed were within the range of similar studies where livestock grazing and mineral fertiliser events occurred in tandem (Hyde et al., 2016; Liang et al., 2018; Mcauliffe et al., 2020; Wecking et al., 2020). The significant interaction ($p < 0.05$) between N_2O measurements by chambers and treatment and time indicates that the timing of management activities affects the rate of N_2O emissions. Similar findings have also been reported by Krol et al. (2017) and Hyde et al. (2016) from the same experimental grounds. Emissions in April accounted for the highest proportion of the total $F_{CH\ FIELD}$ N_2O-N flux and similarly, high instantaneous emission events were recorded by EC

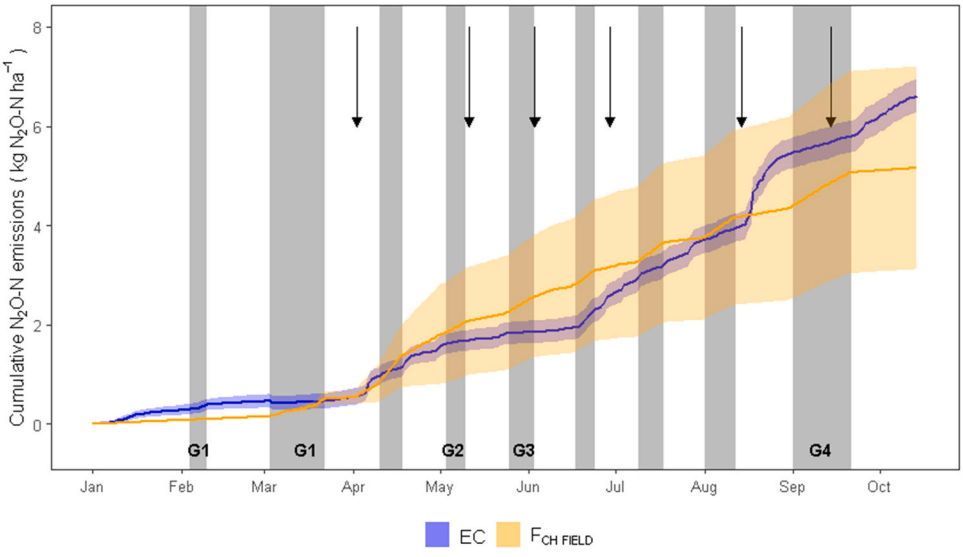

Fig. 3. Field scale cumulative N_2O-N emissions over 288 days by gap-filled eddy covariance (EC) (blue line) and up scaled static chamber ($F_{CH\ FIELD}$) (orange line) and where the blue and orange shades represent the 95% C.I. for EC and chamber measurements, respectively. The grey back drop represents grazing periods where G1–G4 represents grazing events 1–4 that were measured for N_2O flux measurements by static chambers. See Table 1 for dates on management activities. Black arrows mark the date of fertiliser applications. (For interpretation of the references to colour in this figure legend, the reader is referred to the web version of this article.)

Table 3
The proportions of cumulative emissions from each grazing period to the total field scale chamber cumulative ($F_{CH\ FIELD}$). N is the number of days incorporated into the cumulative, which is the period between the start of a grazing event and the beginning of the next grazing event.

Event #	Grazing	N	Cumulative N_2O-N flux kg N ha^{-1}	Proportion of total flux %
Pre-grazing	01/01/2020–03/02/2020	34	0.08	1.63
1	04/02/2020–10/02/2020	28	0.07	1.34
2	03/03/2020–02/04/2020	38	0.65	12.56
3	10/04/2020–18/04/2020	23	1.01	19.67
4	03/05/2020–10/05/2020	22	0.42	8.18
5	25/05/2020–03/06/2020	22	0.52	10.14
6	17/06/2020–24/06/2020	23	0.50	9.61
7	09/07/2020–18/07/2020	23	0.48	9.34
8	01/08/2020–12/08/2020	30	0.60	11.62
9	31/08/2020–21/09/2020	22	0.73	14.20
Post-gazing	22/09/2020–14/10/2020	23	0.09	1.71
Total		288	5.16	100.00

in April. Such high emission events are likely due to denitrification for a number of reasons. Firstly, observations of heavy (> 3 mm) and/or consistent rainfall and subsequently an increasing the WFPS (> 60%), prior to the April emission event as well as moderate soil temperatures (mean 11 ± 1 °C standard deviation) were recorded. It is important to note that all of the above listed environmental variables are key regulators for the production of N_2O by denitrifiers (Butterbach-Bahl et al., 2013). Secondly, WFPS, rainfall and soil temperature were positively and significantly correlated with N_2O-N emissions during this period (Table 2A), further validating the significance of the observations mentioned. An additional stepwise regression analysis merging N_2O-N EF and soil property data measured in this study with data from the same experimental site by Krol et al. (2016) and Maire et al. (2020) also showed that soil moisture drives N_2O emissions from this site (Table 3A). It is worth mentioning, that similar environmental conditions were also recorded during the August N_2O emission peak measured by EC. Finally, N inputs from both urine and dung from grazing animals, and fertiliser N showed high mean concentrations of NH_4^+ and NO_3^- prior to April at 13.7 and 21.4 mg N kg^{-1} soil, respectively, suggesting an availability of N substrates for denitrification during April (Table 4A). The co-occurrence of favourable environmental conditions promoting anoxic conditions in combination with sufficient substrate availability from management, thus creates optimum conditions for the denitrification of NO_3^- to N_2O (Butterbach-Bahl et al., 2013). Overall, these findings suggest that reducing or delaying management activity during wet seasons or periods could potentially reduce annual N_2O emissions i.e. implementing precision management (Rees et al., 2020).

Low N_2O emissions were observed for grazing events in February and March by EC despite coinciding with consistent rainfall and an elevated WFPS (> 60%). In this case, it is likely that the potential for nitrification was reduced as determined by low mean NO_3^- concentrations measured in February and March at 9.5 and 11.0 NO_3^--N mg kg soil, respectively (Table 4A). Additionally, lower soil temperatures (mean 6.7 ± 1.5 °C SD) relative to the rest of the year, could have resulted in changes in the composition of denitrifying communities, potentially limiting the soil microbial production of N_2O emissions (Braker et al., 2010). Furthermore, it is possible that low N_2O emissions were due to available NO_3^- being utilised for N_2 production via codenitrification. Selbie et al. (2015) reported high N losses following urine deposition of 55.8 g N m^{-2} as N_2 by the process of codenitrification. Despite unfavourable conditions for the production of N_2O during this period (G1), high emissions were reported by static chamber measurements. Flux measurements of N_2O by static chambers typically display a log-normal distribution over time which is characterised by a few high flux measurements (Cowan et al., 2015; Hyde et al., 2016; Maire et al., 2020). Due to the limited spatial and temporal resolution of this technique, where high flux values are recorded, static chambers will typically over-estimate the sample mean, and where such values are absent from the dataset, chamber fluxes will underestimate the sample mean (Levy et al., 2017). In this study chamber flux values ranged over five orders of magnitude (Fig. 2A), where the sample mean is weighted towards a few high flux measurements. Due to the small sample size (n = 5 per treatment), it is difficult to constrain the variability and therefore the high uncertainty associated with chamber flux measurements. Previous studies have also reported large spatial differences in chamber N_2O flux measurements. For example, Cowan et al. (2015) measured N_2O fluxes ranging from 2000 to 79,000 μg N_2O-N m^{-2} h^1 over 100 sampling points, from a 7 hectare grazed grassland in Scotland. Similarly, Turner et al. (2008) recorded N_2O fluxes from an Australian irrigated dairy pasture that ranged from 45 to 765 ng N_2O-N m^{-2} s^{-1} in summer and 20–953 ng N_2O-N m^{-2} s^{-1} in autumn. Conversely, the EC technique is cable of integrating both high and low fluxes over large areas (approximately 1 km^2) with constant 24 h measurement coverage, thus providing more certain estimates of field scale emissions of N_2O relative to the static chamber technique. Therefore higher emissions reported by static chambers compared to EC are likely due to its limited spatial and temporal resolution and potential for large interpolation uncertainties, a major disadvantage of static chambers which previous studies have reported on (Cowan et al., 2019; Jones et al., 2011).

4.2. Emission factors of CAN, SU+CAN and dung+CAN

In this study EFs for CAN, SU + CAN and dung + CAN were highly variable over the four grazing events. CAN showed the highest EF relative to the other treatments, with a mean EF of 2.78% (1.60–5.58%). The lower-end CAN emissions observed in this study have also been reported by Cardenas et al. (2019) from four grassland sites in the UK (0.58–1.36%) and Harty et al. (2016) from two different grassland sites in Ireland (1.44 ± 0.90% and 1.67 ± 0.49%). Harty et al. (2016) also reported similar high-end EFs from CAN from an additional grassland site in Ireland at 3.81 ± 0.20% and Velthof and Losada (2011) reported a maximum EF of 8.3% from a grassland site in the Netherlands. The variability in CAN EFs could be explained by soil conditions at the chamber location, with the greatest emissions occurring in grazing 1 in spring where the soil moisture content was predominately high (WFPS > 60%), favouring denitrification (Linn and Doran, 1984), whereas EFs were lower during summer grazing events where soil conditions were relatively drier (WFPS < 60%).

To date, only a few studies have quantified N losses from the interactive effects of CAN applied to urine and dung patches from grazed pastures (Hyde et al., 2016; Krol et al., 2016; Maire et al., 2020). Interactions between fertiliser N and animal excreta create hotspots of N_2O which are a common feature of rotational grazing management (Luo et al., 2017). Currently there are no recommended default EFs by the IPCC or at the national level, for mineral N fertiliser applied to urine or dung patches. In this study, EFs from SU+CAN and dung + CAN were

measured in order to quantify emission events which are representative of rotational grazing systems. The SU+CAN treatment EF was 0.59% (0.28–1.28%) which was approximately four times lower than the combined EF_1 and EF_{3PRP} for cattle urine by the IPCC of 2.37% and Irelands combined Tier 2 $EF_{1\ CAN}$ and $EF_{3cattle\text{-}urine}$ of 2.6%. However, mean EFs for SU+CAN were comparable with previously reported SU + CAN EFs in Ireland, by Maire et al. (2020) at 0.26–0.74% and Krol et al. (2017) at 0.55.%. Hyde et al. (2016) showed a multiplicative effect on cumulative N_2O emissions from CAN and urine applied together, relative to N_2O emissions from these treatments individually. In this study, emissions from SU + CAN showed more of an additive effect where frequently, cumulative N_2O-N losses from SU + CAN were approximately twice that of N_2O-N losses observed from the CAN treatment.

In this study, mean EFs quantified from dung + CAN were 0.64% (0.30–1.01%), which was roughly half of the combined EF_1 and EF_{3PRP} for cattle dung by the IPCC, and Irelands combined Tier 2 inventory value for $EF_{1\ CAN}$ and $EF_{3cattle\text{-}dung}$, both at 1.7%. Few studies have investigated the interactive effects of dung and CAN on N_2O emissions, however Hyde et al. (2016) showed that applying dung and CAN together had additive effects on N_2O emissions, reporting N losses of 2.15%. Cumulative emissions from the dung+CAN treatment were greater than cumulative emissions from the CAN treatment alone for grazing 2 and 3, which could be explained by possible additive effects between treatments. An independent dung treatment however, would be necessary to validate these assumptions. The readily available carbon (C) in dung can increase rates of microbial oxygen consumption, thus creating anaerobic conditions (Van Groenigen et al., 2005). Increased C availability can also accelerate microbial activity as nitrifiers and denitrifiers require readily available C for the oxidation of NH_4^+ and the reduction of NO_3^- (Wang et al., 2021). Additionally, the soil nitrate N pool available from CAN alone was frequently lower than the dung+CAN treatment (Table 4A). This in combination with pre-existing amino-sugars from the dung patch, and high soil moisture, would create optimum conditions for the production of N_2O by either denitrification or co-denitrification, thus increasing emissions (Rex et al., 2018, 2019).

4.3. Field scale grazing N_2O emissions

Total cumulative N_2O-N emissions measured by gap-filled EC and $F_{CH\ FIELD}$ were 6.62 ± 0.33 kg N ha^{-1} and 5.16 ± 2.04 kg N ha^{-1}, which represent a global EF of 0.96% and 0.72%, respectively, and both are similar to mean of the IPCCs default value for EF_1 and EF_{3PRP} at 0.95%. It is important to note that larger disparities between gap-filled EC and $F_{CH\ FIELD}$ cumulative N_2O-N emissions would have been observed if the temporal frequency of static chamber flux measurements were lower. For example, if N_2O flux measurements were not measured during March and April (which accounted for 32.23% of the total $F_{CH\ FIELD}$ emissions [Table 3]), the cumulative N_2O losses calculated from $F_{CH\ FIELD}$ would have been 3.45 kg N ha^{-1}, which is approximately 50% lower than total N_2O emissions measured by EC. Our study highlights the importance of high chamber replication and measurements both spatially and temporally in order to make field scale estimates of N_2O comparable with high frequency N_2O flux measurements by EC. Similar conclusions were also outlined by Murphy et al. (2021), who showed that N_2O flux measurements by static chambers and EC were most comparable when chamber replication was high and when measurements from both techniques displayed temporal and spatial alignment.

Both F_{CH_Field} and EC cumulative emissions were within range for previously reported N_2O-N emissions from intensively grazed dairy pastures. Flechard et al. (2007) reported total emissions of 6.48 kg N_2O-N ha^{-1} using the static chamber technique from a grassland site in the Netherlands which received 300 kg N ha^{-1}. Hörtnagl et al. (2018) quantified cumulative emissions by EC of 2.55 – 7.89 kg N_2O-N ha^{-1} from a grassland site in Switzerland with an N application rate of 232–219 kg N ha^{-1}, while Wecking et al. (2020) reported cumulative N_2O emissions of 3.82 and 7.30 kg N_2O-N ha^{-1} measured by static chambers and EC respectively, from a grazing system in New Zealand which received 40 kg N ha^{-1} from fertiliser and 424 kg N ha^{-1} from animal excreta during grazing.

The uncertainty associated with $F_{CH\ FIELD}$ was approximately seven times greater than the uncertainty attributed to emissions measured by gap-filled EC. The high uncertainty associated with $F_{CH\ FIELD}$ estimates can partly be explained by small sample sizes per treatment (n = 5* treatments per grazing). Studies have shown that where chamber sample sizes are large (n > 40), the uncertainty in chamber flux measurements is reduced (Cowan et al., 2020). However, it is not always practical or feasible to manage high static chamber replications for multiple treatments. Where the sample size is small and the data is both highly variable and exhibits a log-normal distribution, as is frequently the case for N_2O flux datasets (Cowan et al., 2016), conventional arithmetic methods for handling flux data are not sufficient for providing robust estimates of uncertainty. More recently, Bayesian methods have been used to report N_2O EFs and uncertainty from static chamber measurements (Cowan et al., 2020). Bayesian statistics provide more robust estimates of uncertainty relative to arithmetic methods, by explicitly accounting for the log-normal distribution of the dataset and is therefore, less likely to over or underestimate the sample mean and associated uncertainty (Levy et al., 2017). Previous studies have demonstrated the success of the Bayesian method in quantifying the uncertainty of chamber N_2O emissions from single management events (Cowan et al., 2019). However, at present the Bayesian method still requires further development in order to quantify chamber measurements of N_2O from emission events arising from consecutive, multiple management practices. Flechard et al. (2007) reported high uncertainty values of up to 50% in annual flux measurements by static chambers due to the spatial and temporal limitations of the technique. Due to the low temporal and spatial resolution of static chamber measurements relative to the EC technique, static chambers are not suitable for capturing hot moments and hotspots of N_2O due to management, rainfall events and re-wetting of dry soils (Jones et al., 2011).

In this study, gap-filled EC cumulative emissions exceeded $F_{CH\ FIELD}$ estimates following the August fertiliser application and the September grazing, which coincided with heavy rainfall events (sum 35 mm) and high soil temperatures (mean 16.3 °C). Maximum differences between EC and $F_{CH\ FIELD}$ cumulative emissions were 1.09 kg N ha^{-1} during these periods. Our results imply that quantifying N_2O emissions using only the static chamber approach could lead to underestimations of annual N_2O-N flux estimates from grazing systems where climatic conditions favour hotspots and hot moments of N_2O, as the total variability in N_2O emissions may not be captured due to the low spatial and temporal resolution of the static chamber technique.

Cumulative estimates of $F_{CH\ FIELD}$ N_2O-N emissions showed the same total cumulative N_2O-N losses as reported in literature values (Table 4, Fig. 4). This study had consistently higher $F_{CH\ FIELD}$ cumulative estimates across all treatments compared with literature value with the exception of CAN, where emissions were 65.61% lower (difference of 0.98 kg N ha^{-1}) compared to literature values. Emissions from background accounted for 14% (0.71 kg N ha^{-1}) and CAN accounted for 36% (1.87 kg N ha^{-1}) of the total N_2O-N losses reported in this study, while animal excreta accounted for 50% (34% or 1.77 kg N ha^{-1} – urine; 16% or 0.81 kg N ha^{-1} – dung). Voglmeier et al. (2019) also reported high contributions of N_2O-N losses from urine (57%) but reported lower contributions from dung (5%) from an intensively managed grassland in Switzerland. Variability in reported EFs from grazing systems in this study and the literature, may be due to the interactive affects between treatments, which can increase N_2O-N emissions due to enhanced substrate availability and soil moisture (Hyde et al., 2016).

Table 4
Cumulative N_2O-N emissions for background (i.e. no N application), calcium ammonium nitrate (CAN), urine and dung using literature emission factor (EF) values by Krol Harty Krol et al. (2017, 2016, 2016) and Maire et al. (2020), respectively.

Author	Treatment	EF		N applied to field	Cumulative N_2O-N flux	
		%	95%. CI	kg N ha^{-1}	kg N ha^{-1}	95% C.I.
Krol et al. (2017)	Background	–	–	–	0.11	–
Harty et al. (2016)	CAN	1.49	0.71	191	2.85	1.36
Krol et al. (2016)	Dung	0.38	0.31	125	0.39	0.31
Marie et al. (2020)	Urine	0.47	0.10	299	1.41	0.50

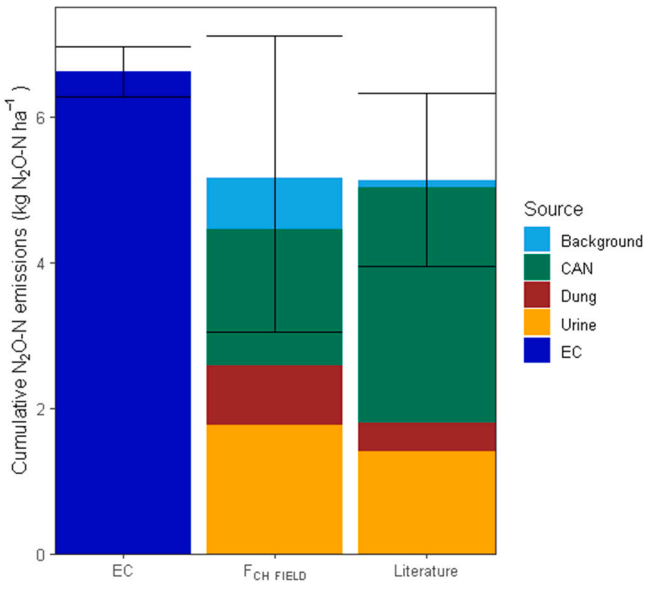

Fig. 4. Cumulative N_2O-N emissions by gap-filled eddy covariance (EC) measurements (dark blue) and upscaled static chamber measurements ($F_{CH\ FIELD}$) for background emissions (light blue), calcium ammonium nitrate (CAN) (green), dung (brown) and urine (orange). Literature values for background, CAN, dung and urine can be seen in Table 4. Error bars represent the 95% confidence interval. (For interpretation of the references to colour in this figure legend, the reader is referred to the web version of this article.)

4.4. Recommendations for future N_2O flux studies

In this study, constant values from the literature were used to quantify the number and area of dung and urine patches per day (Dennis et al., 2011; White et al., 2001; Wilkinson and Lowrey, 1973). The N content of dung and urine is often unknown or is simulated using a constant N content to evaluate the effect of deposition timing on emissions. The N content of urine varies greatly over the season reflecting factors such as the feed N content, feed dry matter, feed and water intake and inter animal differences. To date, there is still a lot of variability surrounding the use of constant values in characterising dung and urine depositions (Aland et al., 2002; Moir et al., 2011; Oudshoorn et al., 2008; Weeda, 1967). Ideally, site specific quantifications of dung and urine deposition events should be made for more accurate estimates of upscaled N_2O emissions from static chamber measurements. For instance, using survey-grade global positioning system (GPS) technology to precisely measure field scale variability in distribution, coverage and diversity of excreta patches (Carpinelli et al., 2020; Dennis et al., 2011; Maire et al., 2018). Furthermore, there is still at large a degree of ambiguity surrounding the probability of overlapping urine or dung patches occurring during grazing, that could potentially lead to greater N losses than individual patches (Cichota et al., 2013; Snow et al., 2017). As a result, there is still a necessity to further our understanding in the variability of N_2O emissions from combined treatments of fertiliser, urine and dung and quantifying dung and urine patches at high precision at the field scale. There is also a need to trial management practices to reduce N_2O emissions such as precision fertilisation and grazing to avoid hot moments (Rees et al., 2020). Additionally, we need more datasets quantifying N_2O emissions and investigating the associated drivers from grazing systems to improve and reduce the uncertainty in modelling EFs from grazed pastures (Tier 3). Improvements in modelling N_2O EFs would in turn avoid the burden of conducting dedicated measurement campaigns for estimating local EFs (López-Aizpún et al., 2020).

5. Conclusion

Quantifying field scale emissions of N_2O in grazed pastures is complicated due to the spatial heterogeneity of dung and urine patches by grazing animals. The EC technique provided spatially and temporally robust annual estimates of N_2O emissions (6.62 ± 0.34 kg N ha^{-1}) from the grazing management, while high uncertainties in emission factor derived chamber cumulative flux ($F_{CH\ FIELD}$) estimates were observed (5.09 ± 2.01 kg N ha^{-1}). Using chamber N_2O flux measurements in a complimentary fashion with N_2O flux measurements made by EC provided insights in the differential contributions of grazing and fertilisation on the field N_2O budget over the grazing season. Management related emissions accounted for 86% of the total cumulative N_2O-N emission, with 50% of N_2O-N losses derived from animal excreta.

Declaration of Competing Interest

The authors declare that they have no known competing financial interests or personal relationships that could have appeared to influence the work reported in this paper.

Acknowledgements

The authors gratefully acknowledge A. Lawless for facilitating the research on the Johnstown Castle Dairy Farm and G. Gillen for gas chromatography analysis. This research was financially supported under the National Development Plan, through the Research Stimulus Fund, administered by the Department of Agriculture, Food and the Marine, Manipulation and Integration of Nitrogen Emissions (MINE) grant number 15S655.

Appendix A. Supporting information

Supplementary data associated with this article can be found in the online version at doi:10.1016/j.agee.2021.107725.

References

Aland, A., Lidfors, L., Ekesbo, I., 2002. Diurnal distribution of dairy cow defecation and urination. Appl. Anim. Behav. Sci. 78, 43–54.
Askew, E., 2012. Inorganic nonmetallic constituents; method 4500-NO 3-H. Automated Hydrazine Reduction Method, 4-128. Stand. Methods Exam. Waters Waste Water 22.
Braker, G., Schwarz, J., Conrad, R., 2010. Influence of temperature on the composition and activity of denitrifying soil communities. FEMS Microbiol. Ecol. 73, 134–148.

Buendia, E., Tanabe, K., Kranjc, A., Baasansuren, J., Fukuda, M., Ngarize, S., Osako, A., Pyrozhenko, Y., Shermanau, P., Federici, S., 2019. Refinement to the 2006 IPCC Guidelines for National Greenhouse Gas Inventories. IPCC, Geneva, Switzerland.
Butterbach-Bahl, K., Baggs, E.M., Dannenmann, M., Kiese, R., Zechmeister-Boltenstern, S., 2013. Nitrous oxide emissions from soils: how well do we understand the processes and their controls? Philos. Trans. R. Soc. B: Biol. Sci. 368, 20130122.
Cardenas, L., Bhogal, A., Chadwick, D., Mcgeough, K., Misselbrook, T., Rees, R., Thorman, R., Watson, C.J., Williams, J., Smith, K., 2019. Nitrogen use efficiency and nitrous oxide emissions from five UK fertilised grasslands. Sci. Total Environ. 661, 696–710.
Carpinelli, S., Da Fonseca, A.F., Weirich Neto, P.H., Dias, S.H.B., Pontes, L.D.S., 2020. Spatial and temporal distribution of cattle dung and nutrient cycling in integrated crop–livestock systems. Agronomy 10, 672.
Chadwick, D., Cardenas, L., Dhanoa, M., Donovan, N., Misselbrook, T., Williams, J., Thorman, R., Mcgeough, K., Watson, C., Bell, M., 2018. The contribution of cattle urine and dung to nitrous oxide emissions: quantification of country specific emission factors and implications for national inventories. Sci. Total Environ. 635, 607–617.
Charteris, A.F., Chadwick, D.R., Thorman, R.E., Vallejo, A., De Klein, C.A., Rochette, P., Cárdenas, L.M., 2020. Global Research Alliance N_2O chamber methodology guidelines: recommendations for deployment and accounting for sources of variability. J. Environ. Qual. 49, 1092–1109.
Cichota, R., Snow, V.O., Vogeler, I., 2013. Modelling nitrogen leaching from overlapping urine patches. Environ. Model. Softw. 41, 15–26.
Clough, T.J., Rochette, P., Thomas, S.M., Pihlatie, M., Christiansen, J.R., Thorman, R.E., 2020. Global research alliance N_2O chamber methodology guidelines: design considerations. J. Environ. Qual. 49, 1081–1091.
Cowan, N., Norman, P., Famulari, D., Levy, P., Reay, D., Skiba, U., 2015. Spatial variability and hotspots of soil N2O fluxes from intensively grazed grassland. Biogeosciences 12, 1585–1596.
Cowan, N., Levy, P., Famulari, D., Anderson, M., Reay, D., Skiba, U., 2017. Nitrous oxide emission sources from a mixed livestock farm. Agric. Ecosyst. Environ. 243, 92–102.
Cowan, N., Levy, P., Drewer, J., Carswell, A., Shaw, R., Simmons, I., Bache, C., Marinheiro, J., Brichet, J., Sanchez-Rodriguez, A., 2019. Application of Bayesian statistics to estimate nitrous oxide emission factors of three nitrogen fertilisers on UK grasslands. Environ. Int. 128, 362–370.
Cowan, N., Levy, P., Maire, J., Coyle, M., Leeson, S., Famulari, D., Carozzi, M., Nemitz, E., Skiba, U., 2020. An evaluation of four years of nitrous oxide fluxes after application of ammonium nitrate and urea fertilisers measured using the eddy covariance method. Agric. For. Meteorol. 280, 107812.
Cowan, N.J., Levy, P.E., Famulari, D., Anderson, M., Drewer, J., Carozzi, M., Reay, D.S., Skiba, U.M., 2016. The influence of tillage on N_2O fluxes from an intensively managed grazed grassland in Scotland. Biogeosciences 13, 4811–4821.
Davidson, E.A., Keller, M., Erickson, H.E., Verchot, L.V., Veldkamp, E., 2000. Testing a conceptual model of soil emissions of nitrous and nitric oxides: using two functions based on soil nitrogen availability and soil water content, the hole-in-the-pipe model characterizes a large fraction of the observed variation of nitric oxide and nitrous oxide emissions from soils. Bioscience 50, 667–680.
De Klein, C., Harvey, M., 2015. Nitrousoxide Chamber Methodology and Guidelines. Ministry for Primary Industry, Wellington, New Zealand.
De Klein, C., Eckard, R., Van Der Weerden, T., 2010. Nitrous oxide emissions from the nitrogen cycle in livestock agriculture: estimation and mitigation. Nitrous Oxide Clim. Change 107–144.
De Klein, C.A., Barton, L., Sherlock, R.R., Li, Z., Littlejohn, R.P., 2003. Estimating a nitrous oxide emission factor for animal urine from some New Zealand pastoral soils. Soil Res. 41, 381–399.
Dennis, S., Moir, J.L., Cameron, K., Di, H., Hennessy, D., Richards, K.G., 2011. Urine patch distribution under dairy grazing at three stocking rates in Ireland. Ir. J. Agric. Food Res. 149–160.
Eggleston, S., Buendia, L., Miwa, K., Ngara, T. , Tanabe, K. 2006. IPCC guidelines for national greenhouse gas inventories.
Flechard, C., Ambus, P., Skiba, U., Rees, R., Hensen, A., Van Amstel, A., Van Den Pol-Van Dasselaar, A., Soussana, J.-F., Jones, M., Clifton-Brown, J., 2007. Effects of climate and management intensity on nitrous oxide emissions in grassland systems across Europe. Agric. Ecosyst. Environ. 121, 135–152.
Forrestal, P.J., Krol, D.J., Lanigan, G., Jahangir, M.M., Richards, K.G., 2017. An evaluation of urine patch simulation methods for nitrous oxide emission measurement. J. Agric. Sci. 155, 725–732.
Fratini, G., Ibrom, A., Arriga, N., Burba, G., Papale, D., 2012. Relative humidity effects on water vapour fluxes measured with closed-path eddy-covariance systems with short sampling lines. Agric. For. Meteorol. 165, 53–63.
Grossi, G., Goglio, P., Vitali, A., Williams, A.G., 2018. Livestock and climate change: impact of livestock on climate and mitigation strategies. Anim. Front. 9, 69–76.
Harty, M.A., Forrestal, P.J., Watson, C., Mcgeough, K., Carolan, R., Elliot, C., Krol, D., Laughlin, R.J., Richards, K.G., Lanigan, G., 2016. Reducing nitrous oxide emissions by changing N fertiliser use from calcium ammonium nitrate (CAN) to urea based formulations. Sci. Total Environ. 563, 576–586.
Haszpra, L., Hidy, D., Taligás, T., Barcza, Z., 2018. First results of tall tower based nitrous oxide flux monitoring over an agricultural region in Central Europe. Atmos. Environ. 176, 240–251.
Haynes, R., Williams, P., 1993. Nutrient cycling and soil fertility in the grazed pasture ecosystem. Adv. Agron. 49, 119–199.
Hörtnagl, L., Barthel, M., Buchmann, N., Eugster, W., Butterbach-Bahl, K., Díaz-Pinés, E., Zeeman, M., Klumpp, K., Kiese, R., Bahn, M., 2018. Greenhouse gas fluxes over managed grasslands in Central Europe. Glob. Change Biol. 24, 1843–1872.
Hutchinson, G.L., Livingston, G.P., 2002. 4.5 Soil–atmosphere gas exchange. In: Methods of Soil Analysis: Part 4 Physical Methods, 5, pp. 1159–1182.
Hyde, B., Forrestal, P.J., Jahangir, M.M., Ryan, M., Fanning, A., Carton, O.T., Lanigan, G., Richards, K.G., 2016. The interactive effects of fertiliser nitrogen with dung and urine on nitrous oxide emissions in grassland. Ir. J. Agric. Food Res. 55, 1–9.
Jarvis, S., Scholefield, D., Pain, B., 1995. Nitrogen cycling in grazing systems. In: Bacon, P.E. (Ed.), Nitrogen fertilization in the environment. Marcel Dekker, New York, pp. 381–419.
Jones, S., Famulari, D., Di Marco, C., Nemitz, E., Skiba, U., Rees, R., Sutton, M., 2011. Nitrous oxide emissions from managed grassland: a comparison of eddy covariance and static chamber measurements. Atmos. Meas. Tech. 4, 2179–2194.
Kaimal, J.C., Finnigan, J.J., 1994. Atmospheric Boundary Layer Flows: Their Structure and Measurement. Oxford University Press.
Kljun, N., Calanca, P., Rotach, M., Schmid, H.P., 2015. A simple two-dimensional parameterisation for Flux Footprint Prediction (FFP). Geosci. Model Dev. 8, 3695–3713.
Kormann, R., Meixner, F.X., 2001. An analytical footprint model for non-neutral stratification. Bound. Layer. Meteorol. 99, 207–224.
Krol, D.J., Carolan, R., Minet, E., Mcgeough, K., Watson, C., Forrestal, P.J., Lanigan, G., Richards, K.G., 2016. Improving and disaggregating N_2O emission factors for ruminant excreta on temperate pasture soils. Sci. Total Environ. 568, 327–338.
Krol, D.J., Minet, E., Forrestal, P.J., Lanigan, G., Mathieu, O., Richards, K.G., 2017. The interactive effects of various nitrogen fertiliser formulations applied to urine patches on nitrous oxide emissions in grassland. Ir. J. Agric. Food Res. 56, 54–64.
Levy, P., Cowan, N., Van Oijen, M., Famulari, D., Drewer, J., Skiba, U., 2017. Estimation of cumulative fluxes of nitrous oxide: uncertainty in temporal upscaling and emission factors. Eur. J. Soil Sci. 68, 400–411.
Liang, L.L., Campbell, D.I., Wall, A.M., Schipper, L.A., 2018. Nitrous oxide fluxes determined by continuous eddy covariance measurements from intensively grazed pastures: temporal patterns and environmental controls. Agric. Ecosyst. Environ. 268, 171–180.
Linn, D.M., Doran, J.W., 1984. Effect of water-filled pore space on carbon dioxide and nitrous oxide production in tilled and nontilled soils. Soil Sci. Soc. Am. J. 48, 1267–1272.
López-Aizpún, M., Horrocks, C.A., Charteris, A.F., Marsden, K.A., Ciganda, V.S., Evans, J. R., Chadwick, D.R., Cárdenas, L.M., 2020. Meta-analysis of global livestock urine-derived nitrous oxide emissions from agricultural soils. Glob. Change Biol. 26, 2002–2013.
Luo, J., Wyatt, J., Van Der Weerden, T.J., Thomas, S.M., De Klein, C.A., Li, Y., Rollo, M., Lindsey, S., Ledgard, S.F., Li, J., 2017. Potential hotspot areas of nitrous oxide emissions from grazed pastoral dairy farm systems. Adv. Agron. 145, 205–268.
Maire, J., Gibson-Poole, S., Cowan, N., Reay, D.S., Richards, K.G., Skiba, U., Rees, R.M., Lanigan, G.J., 2018. Identifying urine patches on intensively managed grassland using aerial imagery captured from remotely piloted aircraft systems. Front. Sustain. Food Syst. 2, 2.
Maire, J., Krol, D., Pasquier, D., Cowan, N., Skiba, U., Rees, R., Reay, D., Lanigan, G.J., Richards, K.G., 2020. Nitrogen fertiliser interactions with urine deposit affect nitrous oxide emissions from grazed grasslands. Agric. Ecosyst. Environ. 290, 106784.
Mcauliffe, G., López-Aizpún, M., Blackwell, M., Castellano-Hinojosa, A., Darch, T., Evans, J., Horrocks, C., Le Cocq, K., Takahashi, T., Harris, P., 2020. Elucidating three-way interactions between soil, pasture and animals that regulate nitrous oxide emissions from temperate grazing systems. Agric. Ecosyst. Environ. 300, 106978.
Misselbrook, T., Cardenas, L., Camp, V., Thorman, R., Williams, J., Rollett, A., Chambers, B., 2014. An assessment of nitrification inhibitors to reduce nitrous oxide emissions from UK agriculture. Environ. Res. Lett. 9, 115006.
Moir, J.L., Cameron, K.C., Di, H.J., Fertsak, U., 2011. The spatial coverage of dairy cattle urine patches in an intensively grazed pasture system. J. Agric. Sci. 149, 473–485.
Moncrieff, J., Clement, R., Finnigan, J., Meyers, T., 2004. Averaging, detrending, and filtering of eddy covariance time series. Handbook of Micrometeorology. Springer.
Murphy, R., Richards, K., Krol, D., Gebremichael, A., Lopez-Sangil, L., Rambaud, J., Cowan, N., Lanigan, G., Saunders, M., 2021. Quantifying nitrous oxide emissions in space and time using static chambers and eddy covariance from a temperate grassland. Copernic. Meet.
O'connell, K., Humphreys, J., Watson, C.J., 2004. Quantification of nitrogen sources for grassland. Winter Sci. Meet. Fertil. Assoc. Irel. 15–28.
Oudshoorn, F.W., Kristensen, T., Nadimi, E.S., 2008. Dairy cow defecation and urination frequency and spatial distribution in relation to time-limited grazing. Livest. Sci. 113, 62–73.
Pachauri, R.K., Allen, M.R., Barros, V.R., Broome, J., Cramer, W., Christ, R., Church, J.A., Clarke, L., Dahe, Q. , Dasgupta, P. 2014. Climate change 2014: synthesis report. Contribution of Working Groups I, II and III to the fifth assessment report of the Intergovernmental Panel on Climate Change, Ipcc.
Peterson, R.A., Cavanaugh, J.E., 2019. Ordered quantile normalization: a semiparametric transformation built for the cross-validation era. J. Appl. Stat. 47, 2312–2327.
Rees, R.M., Maire, J., Florence, A., Cowan, N., Skiba, U., Van Der Weerden, T., Ju, X., 2020. Mitigating nitrous oxide emissions from agricultural soils by precision management. Front. Agric. Sci. Eng. 7, 75–80.
Rex, D., Clough, T.J., Richards, K.G., De Klein, C., Morales, S.E., Samad, M.S., Grant, J., Lanigan, G.J., 2018. Fungal and bacterial contributions to codenitrification emissions of N 2 O and N 2 following urea deposition to soil. Nutr. Cycl. Agroecosyst. 110, 135–149.
Rex, D., Clough, T.J., Richards, K.G., Condron, L.M., De Klein, C.A., Morales, S.E., Lanigan, G.J., 2019. Impact of nitrogen compounds on fungal and bacterial contributions to codenitrification in a pasture soil. Sci. Rep. 9, 1–10.

Roche, L., Forrestal, P., Lanigan, G., Richards, K., Shaw, L., Wall, D., 2016. Impact of fertiliser nitrogen formulation, and N stabilisers on nitrous oxide emissions in spring barley. Agric. Ecosyst. Environ. 233, 229–237.
Rochette, P., 2011. Towards a standard non-steady-state chamber methodology for measuring soil N2O emissions. Anim. Feed Sci. Technol. 166, 141–146.
Rochette, P., Bertrand, N., Carter, M., Gregorich, E., 2008. Soil-surface Gas Emissions. Soil Sampling and Methods of Analysis. CRC Press, Boca Raton, FL, pp. 851–861.
Selbie, D.R., Lanigan, G.J., Laughlin, R.J., Di, H.J., Moir, J.L., Cameron, K.C., Clough, T. J., Watson, C.J., Grant, J., Somers, C., 2015. Confirmation of co-denitrification in grazed grassland. Sci. Rep. 5, 1–9.
Simon, P.L., Dieckow, J., De Klein, C.A., Zanatta, J.A., Van Der Weerden, T.J., Ramalho, B., Bayer, C., 2018. Nitrous oxide emission factors from cattle urine and dung, and dicyandiamide (DCD) as a mitigation strategy in subtropical pastures. Agric. Ecosyst. Environ. 267, 74–82.
Skiba, U., Jones, S., Dragosits, U., Drewer, J., Fowler, D., Rees, R., Pappa, V., Cardenas, L., Chadwick, D., Yamulki, S., 2012. UK emissions of the greenhouse gas nitrous oxide. Philos. Trans. R. Soc. B: Biol. Sci. 367, 1175–1185.
Snow, V.O., Cichota, R., Mcauliffe, R., Hutchings, N.J., Vejlin, J., 2017. Increasing the spatial scale of process-based agricultural systems models by representing heterogeneity: the case of urine patches in grazed pastures. Environ. Model. Softw. 90, 89–106.
Team, R. 2020. RStudio: Integrated Development for R. In: RSTUDIO, P. (ed.). Boston, MA.
Turner, D.A., Chen, D., Galbally, I., Leuning, R., Edis, R., Li, Y., Kelly, K., Phillips, F., 2008. Spatial variability of nitrous oxide emissions from an Australian irrigated dairy pasture. Plant Soil 309, 77–88.
USDA 1999. USDA Soil Quality Test Kit Guide, Washington DC: USA.
Van Der Weerden, T.J., Noble, A., De Klein, C.A., Hutchings, N., Thorman, R.E., Alfaro, M.A., Amon, B., Beltran, I., Grace, P., Hassouna, M., 2021. Ammonia and nitrous oxide emission factors for excreta deposited by livestock and land-applied manure. J. Environ. Qual. 1–19.
Van Groenigen, J.W., Velthof, G.L., Van Der Bolt, F.J., Vos, A., Kuikman, P.J., 2005. Seasonal variation in N_2O emissions from urine patches: effects of urine concentration, soil compaction and dung. Plant Soil 273, 15–27.
Velthof, G.L., Losada, J.M., 2011. Calculation of nitrous oxide emission from agriculture in the Netherlands: update of emission factors and leaching fraction. Alterra.
Vickers, D., Mahrt, L., 1997. Quality control and flux sampling problems for tower and aircraft data. J. Atmos. Ocean. Technol. 14, 512–526.
Voglmeier, K., Six, J., Jocher, M., Ammann, C., 2019. Grazing-related nitrous oxide emissions: from patch scale to field scale. Biogeosciences 16, 1685–1703.
Wang, C., Amon, B., Schulz, K., Mehdi, B., 2021. Factors that influence nitrous oxide emissions from agricultural soils as well as their representation in simulation models: a review. Agronomy 11, 770.
Wecking, A.R., Wall, A.M., Liáng, L.L., Lindsey, S.B., Luo, J., Campbell, D.I., Schipper, L. A., 2020. Reconciling annual nitrous oxide emissions of an intensively grazed dairy pasture determined by eddy covariance and emission factors. Agric. Ecosyst. Environ. 287, 106646.
Weeda, W., 1967. The effect of cattle dung patches on pasture growth, botanical composition, and pasture utilisation. N. Z. J. Agric. Res. 10, 150–159.
White, S., Sheffield, R., Washburn, S., King, L., Green J., J.R., 2001. Spatial and time distribution of dairy cattle excreta in an intensive pasture system. J. Environ. Qual. 30, 2180–2187.
Wilkinson, S., Lowrey, R., 1973. Cycling of mineral nutrients in pasture ecosystems. Chem. Biochem. Herb.